

## L-cysteine-assisted Synthesis of AgInS<sub>2</sub> Microspheres

LIU Hai-Tao<sup>1</sup>, ZHONG Jia-Song<sup>2</sup>, LIANG Xiao-Juan<sup>1</sup>, ZHANG Jing-Feng<sup>1</sup>, XIANG Wei-Dong<sup>1,2</sup>

(1. College of Chemistry and Materials Engineering, Wenzhou University, Wenzhou 325035, China; 2. School of Materials Science and Engineering, Tongji University, Shanghai 200092, China)

**Abstract:** AgInS<sub>2</sub> microspheres were synthesized via a simple solvothermal route using biomolecule L-cysteine-assisted methods. The L-cysteine both as sulfur source and complexing agent plays an important role in the formation of AgInS<sub>2</sub> microspheres. The morphology, structure, and phase composition of the as-prepared AgInS<sub>2</sub> products were studied through X-ray diffraction, field emission scanning electron microscope, energy dispersive X-ray spectroscopy, X-ray photoelectron spectroscopy, transmission electron microscope, and high-resolution transmission electron microscope. The Results showed that the as-prepared AgInS<sub>2</sub> microspheres were orthorhombic phase with average diameters of about 2  $\mu\text{m}$ . In addition, the effect of reaction temperature on morphology of the product was investigated, and a possible growth mechanism of the AgInS<sub>2</sub> microspheres was also determined based on electron microscope.

**Key words:** AgInS<sub>2</sub>; L-cysteine; biomolecule; semiconductor

Ternary chalcogenides of I-III-VI (I=Cu, Ag; III=Ga, In; VI=S, Se, Te) have attracted great research interests due to their excellent electrical and optical properties, and their important technological applications in areas such as photovoltaic solar cells, linear and nonlinear optical devices, and light emitting diodes<sup>[1-2]</sup>. Because their energy band gaps lie between 0.8 eV and 2 eV, ternary chalcogenides semiconductor compounds have also attracted considerable attention in solar energy conversion<sup>[3]</sup>. As one of the most important ternary chalcogenides, AgInS<sub>2</sub> is expected to make good solar cell absorber layer, owing to its large absorption coefficient and band gap energy between 1.87 eV and 2.03 eV<sup>[4]</sup>. Considerable progress has been made in the synthesis of AgInS<sub>2</sub> semiconductor crystallites by different methods such as the Hot-Press (HP) method<sup>[5]</sup>, direct fusion of Ag, In and S elements<sup>[6]</sup>, the vertical gradient freezing (VGF) method<sup>[7]</sup>, the epitaxy method<sup>[8]</sup>, single-source precursor route<sup>[9]</sup>, dual-source precursors method<sup>[10]</sup> and hydrothermal or solvothermal technique<sup>[11]</sup>. However, few reports on a general facile, low-energy spent route to synthesized AgInS<sub>2</sub> crystals have been published. Biomolecule-assisted synthesis method has become a new and promising focus in the preparation of various micro/nanomaterials<sup>[12]</sup>.

Biomolecules, as the basic building blocks of life, have special structures and fascinating self-assembling func-

tions<sup>[13]</sup>. Thus, they have been exploited as structure-directing agents or reactant sources<sup>[14]</sup>. Recently, biomolecule-assisted route has been proved to be a novel, eco-friendly, and promising method for the preparation of various nanomaterials because of its convenience and strong function in morphology control<sup>[15]</sup>. For example, Xie *et al*<sup>[17]</sup> have synthesized the flowerlike Bi<sub>2</sub>S<sub>3</sub><sup>[16]</sup>, nanocube-based pagoda-like PbS, the porous spongy-like Ni<sub>3</sub>S<sub>2</sub><sup>[18]</sup>, and network-like MnS nanostructures<sup>[19]</sup> by biomolecule L-cysteine-assisted methods. Inspired by their work, it is interesting to investigate the preparation and assembly of other sulfide nanomaterials by L-cysteine-assisted biological approaches<sup>[14]</sup>. L-cysteine (Cys, HSCH<sub>2</sub>CH(NH<sub>2</sub>)COOH) is an inexpensive, simple, and environment-friendly thiol-containing amino acid, which serves as both of sulfur source and template in the formation of metal sulfide nanostructures<sup>[20]</sup>. Thus, it is worthy to develop a simple L-cysteine-assisted approach to prepare other sulfide nanomaterials, especially with a novel homogeneous self-assembly pattern of ternary chalcogenide semiconductor nanostructures. To the best of our knowledge, there have no reports on the synthesis of AgInS<sub>2</sub> microspheres using amino acids as the sulfur source to date. Herein, we report an L-cysteine-assisted solvothermal route for the synthesis of AgInS<sub>2</sub> microspheres using L-cysteine as the sulfur source and com-

Received date: 2011-04-06; Modified date: 2011-05-07; Published online: 2011-06-30

Foundation item: National Natural Sciences Foundation of China (50772075, 50972107)

Biography: LIU Hai-Tao(1963–), male, PhD, associate professor.

Corresponding author: XIANG Wei-Dong, professor. E-mail: weidongxiang@yahoo.com.cn

plexing agent. The possible growth mechanism for the formation of AgInS<sub>2</sub> microspheres is preliminarily investigated on the basis of experimental results.

## 1 Experimental

### 1.1 Materials

All of the chemicals are of analytical grade and used without any further purification.

### 1.2 AgInS<sub>2</sub> Microsphere Preparation

In a typical procedure, 1 mmol AgNO<sub>3</sub>, 1 mmol InCl<sub>3</sub> and 2 mmol L-cysteine were dissolved in 40 mL N,N-dimethylformamide (DMF) under constant stirring. After being stirred for 15 min, the mixture was transferred into a Teflon-lined stainless steel autoclave with a capacity of 50 mL. The autoclave was sealed and maintained at 180°C for 24 h and then cooled to room temperature naturally. The precipitates were filtered and washed several times with deionized water and absolute alcohol to remove the residual impurities, and then dried in a vacuum at 55°C for 6 h.

### 1.3 Characterization

The as-prepared samples were characterized by powder X-ray diffraction (XRD) on a Bruker D8-Advance X-ray diffractometer with graphite monochromated Cu K $\alpha$  radiation ( $\lambda = 0.15406$  nm). X-ray photoelectron spectroscopy (XPS) was performed on an ESCALAB 250 X-ray photoelectron spectroscopy, using AlK $\alpha$  X-rays as the excitation source. Field-emission scanning electron microscope (FESEM) images were taken on a JEOL-JSM-6700F scanning electron microscope (10 kV) equipped with an X-ray energy dispersive spectroscopy (EDS) at an accelerating voltage of 20 kV. Transmission electron microscope (TEM) micrograph and the corresponding high-resolution TEM (HRTEM) images were taken on a FEI Tecnai F-20 transmission electron microscopy at an acceleration voltage of 200 kV.

## 2 Results and discussion

The phase characteristics of the as-synthesized products were examined by powder X-ray diffraction (XRD). The XRD pattern shown in Fig. 1 reveals that almost all of the diffraction peaks agree with the orthorhombic AgInS<sub>2</sub> (lattice parameters:  $a=0.7001$  nm,  $b=0.8278$  nm and  $c=0.6698$  nm, JCPDS No. 25-1328). Several other weak peaks which are not indexed belong to minor amount of Ag<sub>2</sub>S crystals (JCPDS No. 01-089-3840) dotted in AgInS<sub>2</sub>.

The surface electronic states and the chemical composition of AgInS<sub>2</sub> microspheres were further confirmed by XPS analysis. No peaks of other elements except Ag, In, S,

C and O are observed in the full XPS spectra (Fig. 2(a)), which indicates the as-prepared sample is highly pure. The peaks at 367.34 eV and 373.42 eV in Fig. 2(b) could be assigned to the binding energies of Ag3d<sub>5/2</sub> and Ag3d<sub>3/2</sub>, respectively<sup>[21]</sup>. The doublet feature of the Ag3d spectrum is due to the spin-orbit separation<sup>[22]</sup>. The two strong peaks at 444.34 eV and 451.85 eV (Fig. 2(c)) can be attributed to binding energies of In3d<sub>5/2</sub> and In3d<sub>3/2</sub>, respectively<sup>[23]</sup>. The peaks at 161.45 eV (Fig. 2(d)) can be assigned to the binding energy of the S2p transition. No obvious impurities could be detected in the sample, which indicates that the level of impurities is lower than the resolution limit of XPS (1at%). The quantification of the peaks gives a Ag:In:S ratio of AgIn<sub>1.02</sub>S<sub>1.98</sub>, which is close to the stoichiometric ratio of AgInS<sub>2</sub>.

The detailed morphology and structure of the products were determined by field emission scanning electron microscope (FESEM). Fig. 3(a) shows the image of the AgInS<sub>2</sub> sample, which indicates that the biomolecule-assisted synthetic route can result in a good yield of microspheres particles and the micro-sized AgInS<sub>2</sub> crystals are as large as about 2  $\mu$ m. The chemical composition of these microspheres was further determined by EDS. Only peaks of the elements Ag, In and S were present in the EDS spectrum (Fig. 3(b)). The atomic ratios are calculated to be 25.05:25.14:49.81 by the comparisons of relative areas under the peaks of Ag, In and S. This result is consistent with the XRD and XPS pattern presented above.

Further structural characterization of AgInS<sub>2</sub> microspheres were carried out by transmission electron microscope (TEM). A typical TEM image of AgInS<sub>2</sub> microspheres structure is shown in (Fig. 4(a)), which reveals a clear and well-defined sphere structure. In addition, the crystallinity of the products was examined by HRTEM. The lattice spacing of 0.356 nm between each adjacent plane is in accordance with the spacing of the (120) crystal

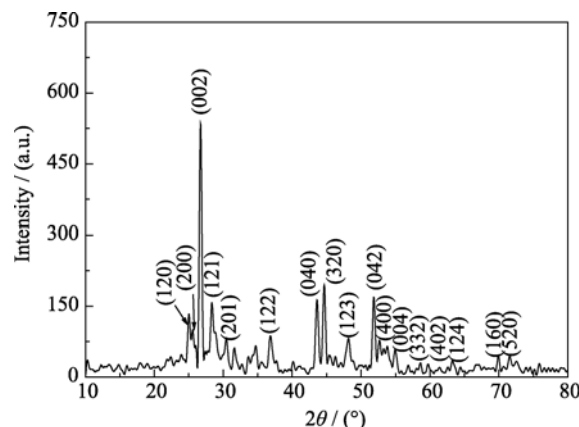
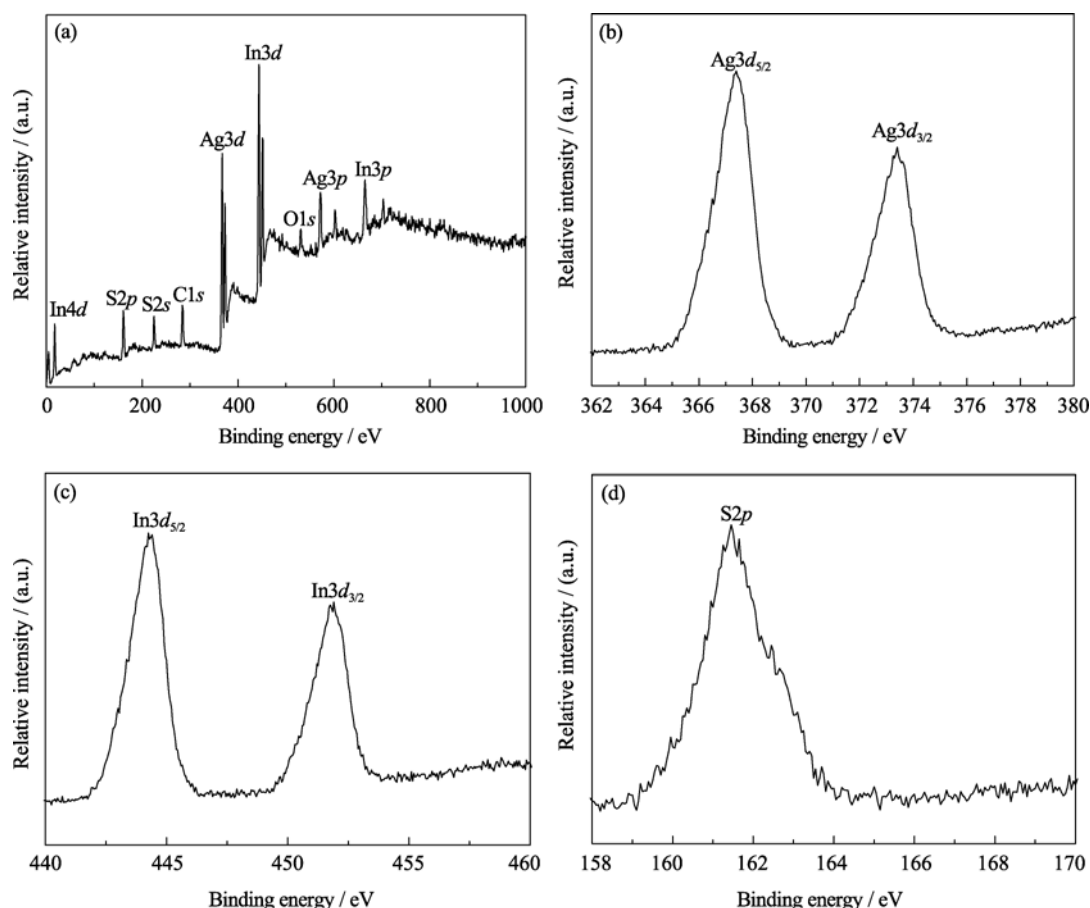
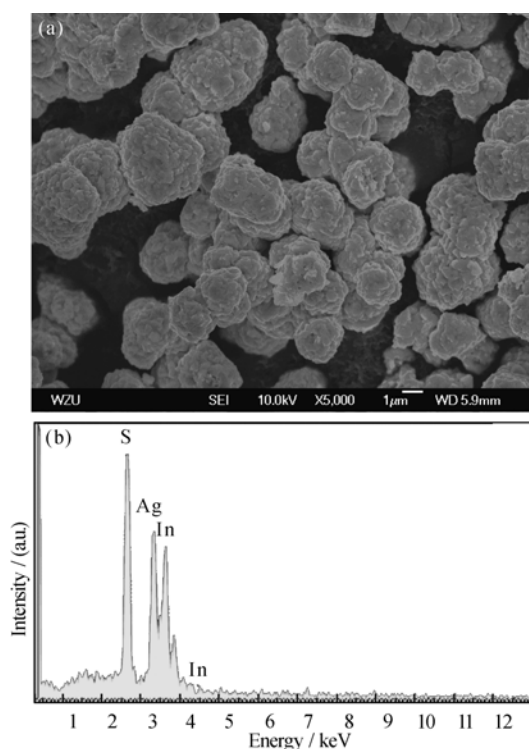


Fig. 1 XRD pattern of AgInS<sub>2</sub> microspheres prepared at 180°C for 24 h

Fig. 2 XPS spectra of the AgInS<sub>2</sub> product

(a) Survey spectrum; (b) Ag3d; (c) In3d; (d) S2p

Fig. 3 (a) FESEM image and (b) EDS spectrum of the as-synthesized AgInS<sub>2</sub> microspheres

planes of orthorhombic AgInS<sub>2</sub>, which agrees well with the (120) *d* spacing of the literature value (JCPDS No. 25-1328).

To investigate the influence of temperature on the morphology, we considered the reaction times as constant factors. It was found that temperature significantly affected the shape and size of the products. AgInS<sub>2</sub> phase can not be obtained at temperature below 140°C but that unidentified amorphous phases are formed. The crystal phase of AgInS<sub>2</sub> was unchanged throughout the reaction from 160°C to 240°C for 24 h. FESEM images of the products obtained at different temperatures are shown in Fig. 5. When the temperature was decreased to 160°C, the irregular spheres-like and nanoparticles were coexisted in the sample, as shown in (Fig. 5(a)). When the temperature increased to 180°C, the FESEM image (Fig. 5(b)) reveals that the irregular sphere-like structure has changed to regular sphere-like structure and irregular nanoparticles were disappear. However, when the temperature increased to 220°C, the microspheres structure has grown too large to disassemble (Fig. 5(c)). As the reaction temperature continued to rise to 240°C, the spherical structure completely disappear (Fig. 5(d)), and the shape of the products

was obviously different from that observed at 160°C, 180°C and 220°C. Therefore, with the temperature rising, the average size of the products is increased and microspheres structure gradually forms, and when the temperature rise to 240°C, the microspheres structure disappears.

On the basis of the experimental results, the probable mechanism of the formation of AgInS<sub>2</sub> microspheres is proposed. In the L-cysteine molecule, there are many functional groups such as amine (–NH<sub>2</sub>), carboxyl (–COOH), and mercaptan (–SH) what have strong tendency to coordinate with inorganic cations and metals to form complex, which has been confirmed by Burford and co-workers on the basis of mass spectrometry<sup>[24]</sup>. Therefore, it is reasonable to conclude that silver ions and indium ions can coordinate with L-cysteine to form initial precursor complexes in our approach. Moreover, it is possible that the amino group reacts with the carboxyl group of the neighboring L-cysteine molecule to form a dipeptide or polypeptide that can serve as the template to form AgInS<sub>2</sub> nanomaterials with various interesting morphologies. So, when mixing the L-cysteine, AgNO<sub>3</sub> and InCl<sub>3</sub> in solution, Ag<sup>+</sup> and In<sup>3+</sup> can coordinate with L-cysteine molecules to form precursor complexes. With increased reaction time, the strong coordination bonds between the hydrosulfide group and Ag<sup>+</sup> and In<sup>3+</sup> could weaken the S–H bond and further break it due to the high reaction temperature. In aqueous solution, due to the interaction of

hydrogen bonds, some primary AgInS<sub>2</sub> nuclei were

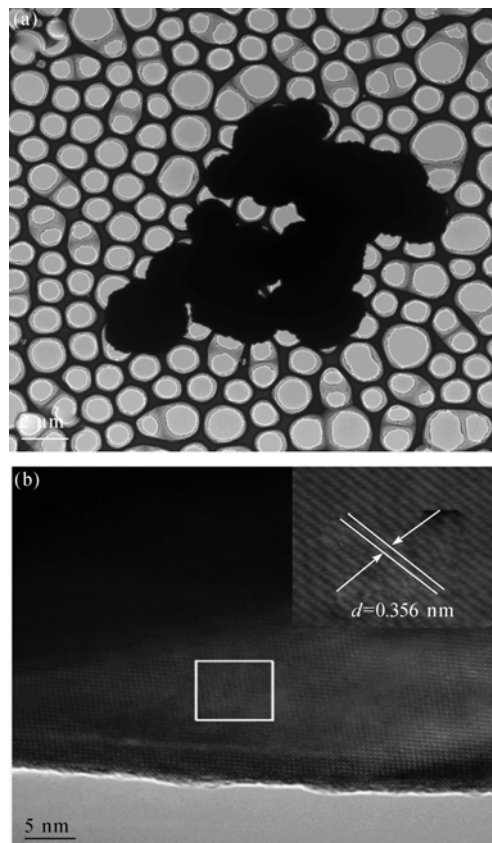


Fig. 4 TEM (a) and HRTEM (b) images of AgInS<sub>2</sub> microspheres

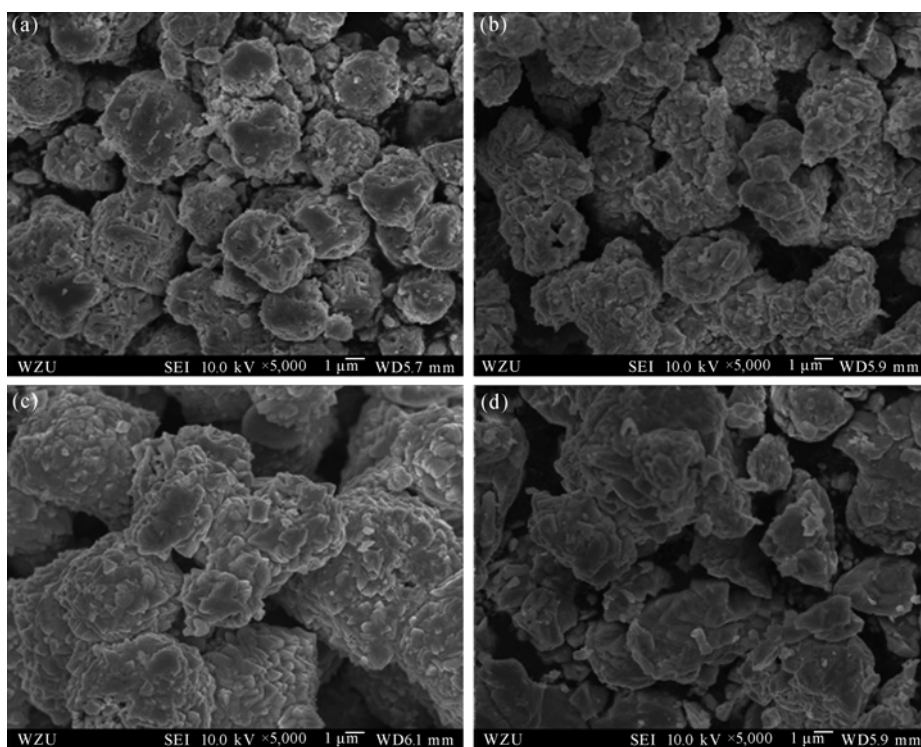
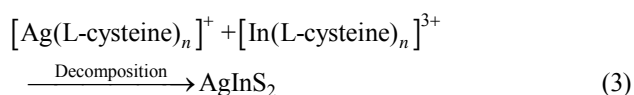
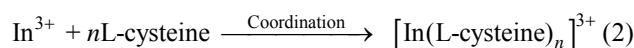
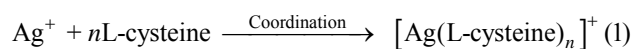


Fig. 5 FESEM images of AgInS<sub>2</sub> products prepared at various temperatures (a) 160°C; (b) 180°C; (c) 220°C; (d) 240°C

formed while elevating the reaction temperature to 200°C. The initial nuclei rapidly aggregated into sphere-like particles, and the particles served as seeds and grew larger. After a period of rapid growth, the small AgInS<sub>2</sub> sphere-like particles could aggregate together to produce AgInS<sub>2</sub> microspheres. A possible formation mechanism of the microspheres nanostructures and their evolution are described as follows:



### 3 Conclusions

A simple biomolecule-assisted solvothermal route has been developed to prepare orthorhombic AgInS<sub>2</sub> microspheres at 180°C for 24 h based on the reactions among AgNO<sub>3</sub>, InCl<sub>3</sub> and L-cysteine in DMF. During the experiments, L-cysteine played an important role in the forming of AgInS<sub>2</sub> microspheres both as sulfur source and complexing agent. XRD and XPS indicated that the pure orthorhombic phase AgInS<sub>2</sub> has been synthesised. FESEM and TEM images showed the AgInS<sub>2</sub> microspheres with a diameter of about 2 μm. EDS analysis gave the atomic ratio of Ag:In:S as 25.05:25.14:49.81 which confirmed the formation of stoichiometric ratio AgInS<sub>2</sub>. The formation mechanism of AgInS<sub>2</sub> microspheres was discussed based on the experimental results. The L-cysteine-assisted solvothermal route provides an alternative approach to generate other ternary sulfide nanocrystals.

### References:

- [1] Yoshino K, Ikari T, Shirakata S, *et al.* Sharp band edge photoluminescence of high-purity CuInS<sub>2</sub> single crystals. *Appl. Phys. Lett.*, 2001, **78**(6): 742–745.
- [2] Lin L H, Wu C C, Lai C H, *et al.* Controlled deposition of silver indium sulfide ternary semiconductor thin films by chemical bath deposition. *Chem. Mater.*, 2008, **20**(13): 4475–4483.
- [3] Chang C C, Liang C J, Cheng K W. Physical properties and photo-response of Cu-Ag-In-S semiconductor electrodes created using chemical bath deposition. *Sol. Energy Mater. Sol. Cells*, 2009, **93**(8): 1427–1434.
- [4] Tian L, Vittal J J. Synthesis and characterization of ternary AgInS<sub>2</sub> nanocrystals by dual- and multiple-source methods. *New J. Chem.*, 2007, **31**(12): 2083–2087.
- [5] Yoshino K, Komaki H, Kakeno T, *et al.* Growth and characterization of p-type AgInS<sub>2</sub> crystals. *J. Phys. Chem. Solids*, 2003, **64**(9/10): 1839–1842.
- [6] Delgado G, Mora A J, Pineda C, *et al.* Simultaneous Rietveld refinement of three phases in the Ag-In-S semiconducting system from X-ray powder diffraction. *Mater. Res. Bull.*, 2001, **36**(13/14): 2507–2517.
- [7] Yoshino K, Mitani N, Sugiyama M, *et al.* Optical and electrical properties of AgIn(SSe)<sub>2</sub> crystals. *Physica B*, 2001, **302–303**: 349–356.
- [8] You S H, Lee K J, Jeong T S, *et al.* Temperature dependence of band gap and photocurrent properties for the AgInS<sub>2</sub> epilayers grown by hot wall epitaxy. *J. Cryst. Growth*, 2002, **245**(3/4): 261–266.
- [9] Tian L, Elim H I, Ji W, *et al.* One-pot synthesis and third-order nonlinear optical properties of AgInS<sub>2</sub> nanocrystals. *Chem. Commun.*, 2006(41): 4276–4278.
- [10] Tian L, Vittal J J. Synthesis and characterization of ternary AgInS<sub>2</sub> nanocrystals by dual- and multiple-source methods. *New J. Chem.*, 2007, **31**(12): 2083–2087.
- [11] Wang D S, Zheng W, Hao C H, *et al.* General synthesis of I–III–VI<sub>2</sub> ternary semiconductor nanocrystals. *Chem. Commun.*, 2008(22): 2556–2558.
- [12] Lei Y Q, Song S Y, Fan W Q, *et al.* Facile synthesis and assemblies of flowerlike SnS<sub>2</sub> and In<sup>3+</sup>-doped SnS<sub>2</sub>: hierarchical structures and their enhanced photocatalytic property. *J. Phys. Chem. C*, 2009, **113**(4): 1280–1285.
- [13] Lu Q, Gao Y F, Komarneni S. Biomolecule-assisted synthesis of highly ordered snowflake-like structures of bismuth sulfide nanorods. *J. Am. Chem. Soc.*, 2004, **126**(1): 54–55.
- [14] Liu S Z, Xiong S L, Bao K Y, *et al.* Shape-controlled preparation of PbS with various dendritic hierarchical structures with the assistance of L-methionine. *J. Phys. Chem. C*, 2009, **113**(30): 13002–13007.
- [15] Qu X F, Zhou G T, Yao Q Z, *et al.* Aspartic-acid-assisted hydrothermal growth and properties of magnetite octahedrons. *J. Phys. Chem. C*, 2010, **114**(1): 284–289.
- [16] Zhang B, Ye X C, Xie Y, *et al.* Biomolecule-assisted synthesis and electrochemical hydrogen storage of Bi<sub>2</sub>S<sub>3</sub> flowerlike patterns with well-aligned nanorods. *J. Phys. Chem. B*, 2006, **110**(18): 8978–8985.
- [17] Zuo F, Yan S, Zhang B, *et al.* L-cysteine-assisted synthesis of PbS nanocube-based pagoda-like hierarchical architectures. *J. Phys. Chem. C*, 2008, **112**(8): 2831–2835.
- [18] Zhang B, Ye X C, Dai W, *et al.* Biomolecule-assisted synthesis and

- electrochemical hydrogen storage of porous spongelike  $\text{Ni}_3\text{S}_2$  nanostructures grown directly on nickel foils. *Chem. Eur. J.*, 2006, **12**(8): 2337–2342.
- [19] Zuo F, Zhang B, Tang X Z, *et al.* Porous metastable  $\gamma\text{-MnS}$  networks: biomolecule-assisted synthesis and optical properties. *Nanotechnology*, 2007, **18**(21): 215608.
- [20] Xiang J H, Cao H Q, Wu Q Z, *et al.* L-cysteine-assisted self-assembly of complex PbS structures. *Cryst. Growth Des.*, 2008, **8**(11): 3935–3940.
- [21] Wagner C D, Riggs W M, Davis L E, *et al.* Handbook of X-ray Photoelectron Spectroscopy. Eden Prairie, MN: Perkin-Elmer Corp, 1978.
- [22] Xiang J H, Cao H Q, Wu Q Z, *et al.* L-cysteine-assisted synthesis and optical properties of  $\text{Ag}_2\text{S}$  nanospheres. *J. Phys. Chem. C*, 2008, **112**(10): 3580–3584.
- [23] Pan D C, An L J, Sun Z M, *et al.* Synthesis of Cu-In-S ternary nanocrystals with tunable structure and composition. *J. Am. Chem. Soc.*, 2008, **130**(17): 5620–5621.
- [24] Burford N, Eelman M D, Mahony D E, *et al.* Definitive identification of L-cysteine and glutathione complexes of bismuth by mass spectrometry: assessing the biochemical fate of bismuth pharmaceutical agents. *Chem. Commun.*, 2003(1): 146–147.

## L-半胱氨酸辅助合成 $\text{AgInS}_2$ 微球

刘海涛<sup>1</sup>, 钟家松<sup>2</sup>, 梁晓娟<sup>1</sup>, 张景峰<sup>1</sup>, 向卫东<sup>1,2</sup>

(1. 温州大学 化学与材料工程学院, 温州 325035; 2. 同济大学 材料科学与工程学院, 上海 200092)

**摘要:** 通过简单的生物分子辅助溶剂热法, 成功地合成出了  $\text{AgInS}_2$  微球. 在反应过程中, 生物分子 L-半胱氨酸既作为硫源也作为络合剂. 利用 X 射线衍射(XRD)、能量色散谱(EDS)、X 射线光电子能谱(XPS)、扫描电子显微镜(SEM)、透射电子显微镜(TEM)等分别对所合成的  $\text{AgInS}_2$  的表面形貌、组成和晶型结构等进行了表征. 结果表明, 所合成的产物为典型的  $\text{AgInS}_2$  正交结构, 平均直径约为 2  $\mu\text{m}$ . 讨论了不同温度对  $\text{AgInS}_2$  的形成及其形貌的影响, 并根据实验结果对所合成的  $\text{AgInS}_2$  微球可能的形成机理进行了简单的探讨.

**关键词:**  $\text{AgInS}_2$ ; L-半胱氨酸; 生物分子; 半导体

中图分类号: O611; TB383

文献标识码: A